Numerical database of highly-resolved turbulent flame-wall interaction simulations for model validation

T. Zirwes[1,2*], F. Zhang[2], M. Steinhausen[3], P. Habisreuther[2], H. Bockhorn[2], C. Hasse[3] and D. Trimis[2]

*thorsten.zirwes@kit.edu

[1] *Steinbuch Centre for Computing, Karlsruhe Institute of Technology, Hermann-von-Helmholtz-Platz 1, 76344 Eggenstein-Leopoldshafen, Germany*

[2] *Engler-Bunte-Institute/Combustion Technology, Karlsruhe Institute of Technology, Engler-Bunte-Ring 7, 76131, Karlsruhe, Germany*

[3] *Simulation of Reactive Thermo-Fluid Systems, Technical University of Darmstadt, Otto-Berndt-Str. 2, 64287, Darmstadt, Germany*

Abstract

The interaction of flames with walls and subsequent flame quenching can be a major cause of pollutant formation in many practical combustion applications. Because of this, a better understanding of flame-wall interaction phenomena is required to optimize future combustion systems. In this work, direct numerical simulations (DNS) are used to study flame-wall interaction of a stoichiometric methane-air flame in a turbulent channel flow. The simulation employs finite rate chemistry and a computational mesh with 200 million cells to resolve the flame-wall interaction without turbulence and combustion model assumptions. The turbulent flow is generated from a separate inert channel flow DNS with periodic boundary conditions. The inert channel flow simulation and the reactive flame-wall interaction simulation are run on the HoreKa cluster at the Karlsruhe Institute of Technology (KIT) and the Hawk supercomputer at the High Performance Computing Center Stuttgart (HLRS) on up to 32768 CPU cores. The simulation results are compiled into a numerical database, containing full three-dimensional data as well as sampling of flame and turbulence properties on two-dimensional cutting planes and one-dimensional lines for model validation. In total, the database consists of 3.5 TB of data. The DNS resolves the smallest length scales in the turbulence-flame-wall interaction zone, so that the database is suitable for developing advanced turbulent combustion models considering the effect of FWI.

Introduction

As emission limits for internal combustion engines become stricter, it is mandatory to increase the efficiency and reduce the formation of pollutants like carbon monoxide and soot. One trend for increasing efficiency is downsizing. However, this typically increases the ratio of wall surface area to volume, leading to intensified flame-wall interaction. As a flame propagates toward a cold wall, it loses heat and eventually quenches [1]. This incomplete combustion process produces increased pollutant levels. Because a better understanding of flame-wall interaction phenomena is required, it has been investigated experimentally [2-5] and numerically [6-9] in the past. However, a reliable and efficient way of describing flame-wall interaction in numerical simulations is still needed. The detailed investigation of flame-wall interaction is difficult because of the small length scales involved, as the flame-wall interaction typically occurs in the sub-millimeter scale. Resolving this near-wall region sufficiently, together with using finite rate chemistry which can introduce chemical time scales that differ by ten orders of magnitude, means that the computational cost is very high.

Because of this, a direct numerical simulation (DNS) of a turbulent channel flow, where a stoichiometric methane-air flame interacts with a cold wall, is performed on one of Germany's fastest supercomputers HPE Apollo Hawk. For the DNS, an in-house code is employed that is based on the open-source computational fluid dynamics library OpenFOAM [10], and has been modified to allow the computation of detailed molecular transport properties [11] and efficient evaluation of chemical reaction rates. The DNS of flame-wall interaction for a V-shaped flame stabilized in a rectangular channel is split into two parts:

- the DNS of the non-reactive turbulent channel flow, which is used to generate turbulent inflow conditions for fully developed turbulent channel flow;
- a subsequent reactive DNS, where a cylindrical flame holder near the inlet creates a V-shaped flame. The lower branch of that flame then interacts with the cold wall at the bottom of the channel.

The second reactive DNS uses the flow field from the first DNS as input for inlet boundary conditions and resolves the FWI zone, turbulent Kolmogorov scale, as well as the flame thickness with at least 15 cells, which allows an in-depth study of turbulence-flame-wall interaction. Focus of the work lies on introducing the DNS database, not on a detailed description of the FWI mechanisms, which will be covered in detail in future works.

Simulation Method

For the simulation of flame-wall interaction in turbulent flows, the fully compressible Navier-Stokes equations are solved. This includes the conservation of total mass

$$\frac{\partial \rho}{\partial t} + \nabla \cdot (\rho \vec{u}) = 0 \tag{1}$$

where ρ is the density, t is time and $\vec{u}$ is the bulk fluid velocity. The conservation of momentum is expressed as

$$\frac{\partial (\rho \vec{u})}{\partial t} + \nabla \cdot (\rho \vec{u} \vec{u}) = -\nabla p + \nabla \cdot \tau \tag{2}$$

where p is the pressure and τ the stress tensor

$$\boldsymbol{\tau} = \mu \left(\nabla \vec{u} + \nabla \vec{u}^{\mathrm{T}} - \frac{2}{3} \nabla \cdot \vec{u} \boldsymbol{I} \right) \tag{3}$$

with μ being the dynamic viscosity of the reacting mixture and $\boldsymbol{I}$ the unit tensor. The conservation of species masses is expressed in terms of the mass fractions Y_k of species *k*:

$$\frac{\partial (\rho Y_k)}{\partial t} + \nabla \cdot (\rho \vec{u} Y_k) = \dot{\omega}_k - \nabla \cdot \vec{j}_k \tag{4}$$

$\dot{\omega}_k$ is the reaction rate of species *k* and $\vec{j}_k$ its diffusive mass flux. The diffusive mass flux in this case is computed by assuming a unity Lewis number

$$\vec{j}_k = -\rho a \nabla Y_k \tag{5}$$

where a is the thermal diffusivity of the gas mixture. Lastly, the conservation of energy is expressed in terms of the total sensible enthalpy:

$$\frac{\partial (\rho (h_s + \frac{1}{2} \vec{u} \cdot \vec{u}))}{\partial t} + \nabla \cdot (\rho \vec{u} (h_s + \frac{1}{2} \vec{u} \cdot \vec{u})) = -\nabla \cdot \vec{q} + \frac{\partial p}{\partial t} - \sum_k h_k^\circ \dot{\omega}_k \tag{6}$$

h_k° is the enthalpy of formation of species k and h_s the sensible enthalpy of the mixture and $\vec{q}$ the diffusive heat flux computed from

$$-\nabla \cdot \vec{q} = \nabla \cdot \lambda \nabla T - \sum_k \nabla \cdot h_{s,k} \vec{j}_k \tag{7}$$

where λ is the heat conductivity of the mixture, T the temperature and $h_{s,k}$ the sensible enthalpy of species k.

The governing equations shown above are solved with the finite volume method (FVM). All spatial derivatives are discretized with a fourth order interpolation method and time derivatives are discretized with an implicit second order backward scheme. Transport coefficients like heat conductivity and thermal diffusivity are computed by the open-source library Cantera [12]. The open-source library Sundials [13] is used to integrate the chemical reaction rates over the simulation time step to decouple the fast chemical time scales from the flow time scales. The in-house code has been validated in previous works and applied to different physical setups [14-27].

The reaction rate $\dot{\omega}_k$ in Eq. (4) has been calculated based on detailed chemistry with Arrhenius' law, which is computationally expensive. To enable the large-scale DNS presented in this work, several performance optimization techniques are included in the in-house code that reduce the time required to compute chemical reaction rates. These performance optimizations include an automated code generation approach to obtain highly optimized machine code [28,29,30] and a load balancing approach that specifically targets the computation of chemical reaction rates [31]. Additionally, the I/O performance of the code has been optimized by utilizing specific cluster hardware [32]. In total, these optimizations can reduce total simulation times by up to 90 % compared to OpenFOAM's standard implementations.

Non-reactive Turbulent Channel Flow

The incompressible DNS of the non-reactive turbulent channel flow case is conducted to generate realistic inflow conditions for the subsequent reactive flame-wall interaction DNS. The computational setup for the channel flow considers a channel with a length of 14 cm, a height of 2 cm and a width of 3 cm. All boundaries are periodic except for the top and bottom wall. A pressure gradient is adaptively set to ensure a bulk velocity of 4.44 m/s. This corresponds to a Reynolds number of $Re = 2770$ with respect to the half channel height and bulk velocity. In total, the mesh consists of 61 million hexahedral cells on a block structured mesh. The mesh is refined toward the walls, where the smallest resolution in wall-normal direction is 25 µm. In the wall-near region, the Kolmogorov length is about 45 µm.

The channel domain together with an iso-surface of the q-criterion from an instantaneous snapshot of the simulation is shown in Figure 1. Every 3 µs, the velocity field on a two-dimensional cutting plane is written to the hard drives, which then serve as inflow condition for the reactive DNS.

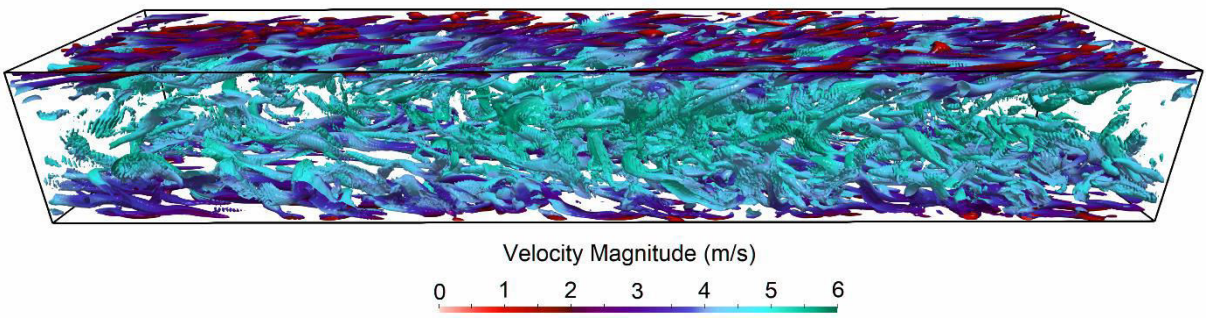

Figure 1. Instantaneous turbulent flow structures visualized by the q-criterion.

Reactive Turbulent Channel Flow

The computational domain of the reactive DNS is similar to the non-reactive case, except that the resolution is finer and the channel is shorter, having a total length of 10 cm. The methane-air mixture at an equivalence ratio of unity enters the domain with a temperature of 300 K. The pressure is atmospheric. Near the inlet, a cylindrical region with a fixed temperature of 2000 K ignites the gas and serves as a flame anchor, creating the V-shaped flame shown in Figure 2. The lower branch of the V-shaped flame then interacts with the cold wall at the bottom of the channel, which has a constant temperature of 300 K, and thus leads to local flame quenching. The turbulent flow generated from the previous non-reacting simulation enters the domain through the inlet on the left.

The mesh consists of 200 million cells, refined toward the bottom wall, with a minimum cell width in wall-normal direction of 12 µm. The employed reaction mechanism is based on the CRECK model [33] and includes 24 chemical species and 165 chemical reactions. To obtain time-averaged quantities, the simulation has been carried out for twenty flow-through times or about 0.5 s.

Because of the large number of computational cells to ensure a good resolution of the flame structure during the flame-wall interaction, this type of simulation is only possible on large supercomputers. Therefore, the simulation has been performed on 32768 CPU cores on one of Germany's largest supercomputers, HPE Apollo Hawk. In total, the simulations of the non-reactive and the reactive channel flow setup have required about 18 million CPU core hours.

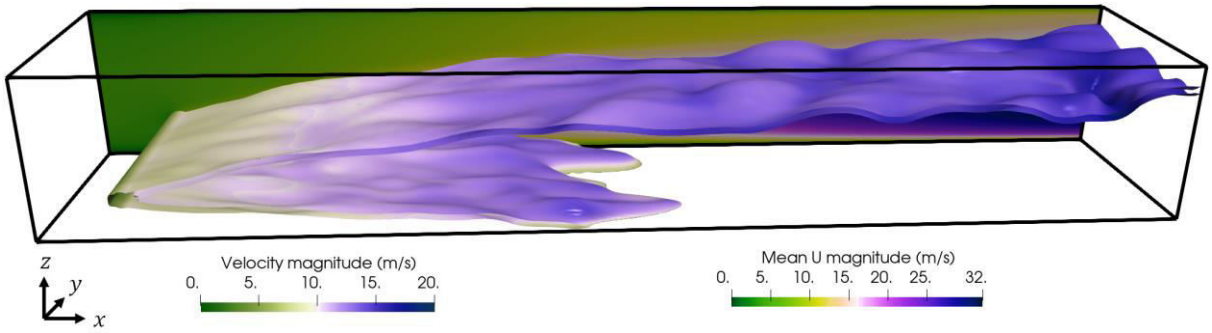

Figure 2. Computational domain for the reacting DNS. Depicted is an instantaneous iso-surface of heat release rate, colored by fluid velocity. In the background, the time averaged velocity field is shown.

Code Performance

Because the large-scale parallel DNS described in the previous sections are only possible on large supercomputers, a good code performance is mandatory. Because of this, a scaling test for the reactive channel flow case has been performed on the supercomputer HoreKa at the Steinbuch Centre for Computing (SCC) at the Karlsruhe Institute of Technology (KIT). Figure 3 shows the strong scaling results, where the base case has been run on 4096 CPU cores and the final simulation runs have been performed with 32768 CPU cores. The numbers in the plot show the parallel scaling efficiency. Even with 32768 CPU cores, the parallel scaling efficiency is nearly at 90 %, demonstrating that the in-house simulation code is able to efficiently handle these types of large parallel simulation cases.

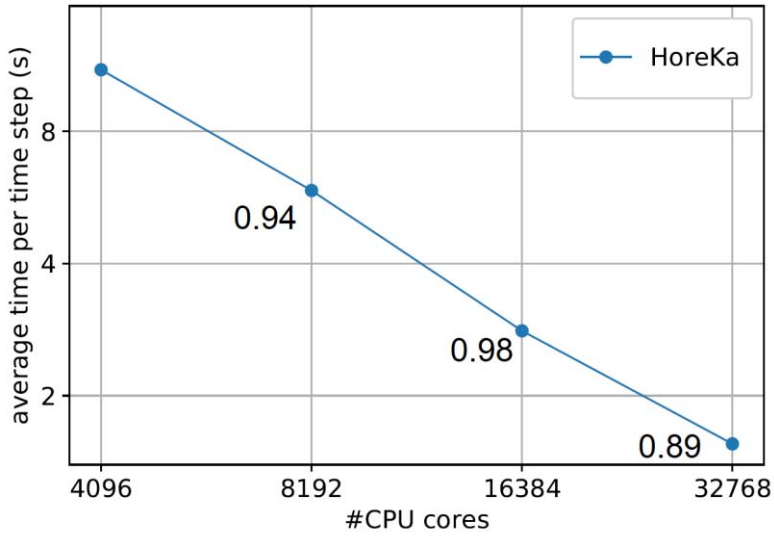

Figure 3. Strong scaling results on the supercomputer HoreKa for the reactive flow simulation.

Numerical Database

The database created from the reactive DNS consists of about 3.5 TB of data. Most of the data volume is comprised of full three-dimensional solution fields. In total, about 2.6 TB, or 25 time steps taken every 10 ms, are available. They contain the mass fractions of all species, temperature, density, their instantaneous, mean and rms values, as well as the chemical reaction rates of all species. Additionally, mixture properties like isobaric heat capacity, heat conductivity, viscosity and absolute enthalpy are available, too. Lastly, since the focus of the case is to provide validation data for flame-wall interaction, the heat fluxes at the cold wall at the bottom of the channel are included in the database.

In addition to the full three-dimensional solution fields, about 8000 two-dimensional cutting planes (800 GB) parallel to the cold wall at the bottom of the channel at different heights are sampled, containing the same quantities as the three-dimensional fields described above. The cutting planes are generated every 0.25 ms. An example of a cutting plane of the temperature field is given in Figure 4. Lastly, the quantities are also sampled every 0.25 ms along 70 one-dimensional lines at different positions and different orientation.

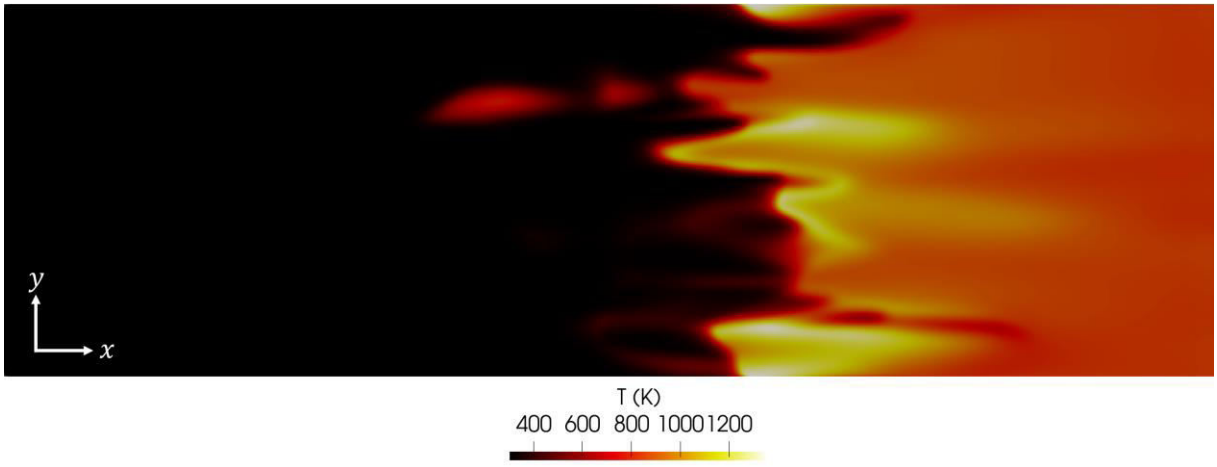

Figure 4. Instantaneous temperature field on a cutting plane parallel to the cold bottom wall in a distance of $z = 2$ mm to the bottom wall.

Flame-wall Interaction

Figure 5 shows the instantaneous flame shape as well as time averaged solution fields on a two-dimensional cutting plane in the $x - z$ plane (see Figure 2) in a region near the bottom wall of the channel. In Figure 5a, the instantaneous temperature field illustrates the wrinkled surface of the flame due to the interaction of with the turbulent flow. The time-averaged temperature field in Figure 5b shows the smooth shape of the V-shaped flame. The thin reaction zone of the flame is illustrated by the reaction rate of CO_2 in Figure 5c. Near the bottom wall, the region marked with the red box is where the flame wall interaction occurs. As shown by the carbon dioxide reaction rate, the flame quenches in close vicinity to the cold wall. The time-averaged field of the CO_2 reaction rate is shown in Figure 5d.

The turbulent flow field can be seen in Figure 5e from the instantaneous values of the stress tensor from Eq. (3), which is homogenized in the high temperature regions created by the burnt gases.

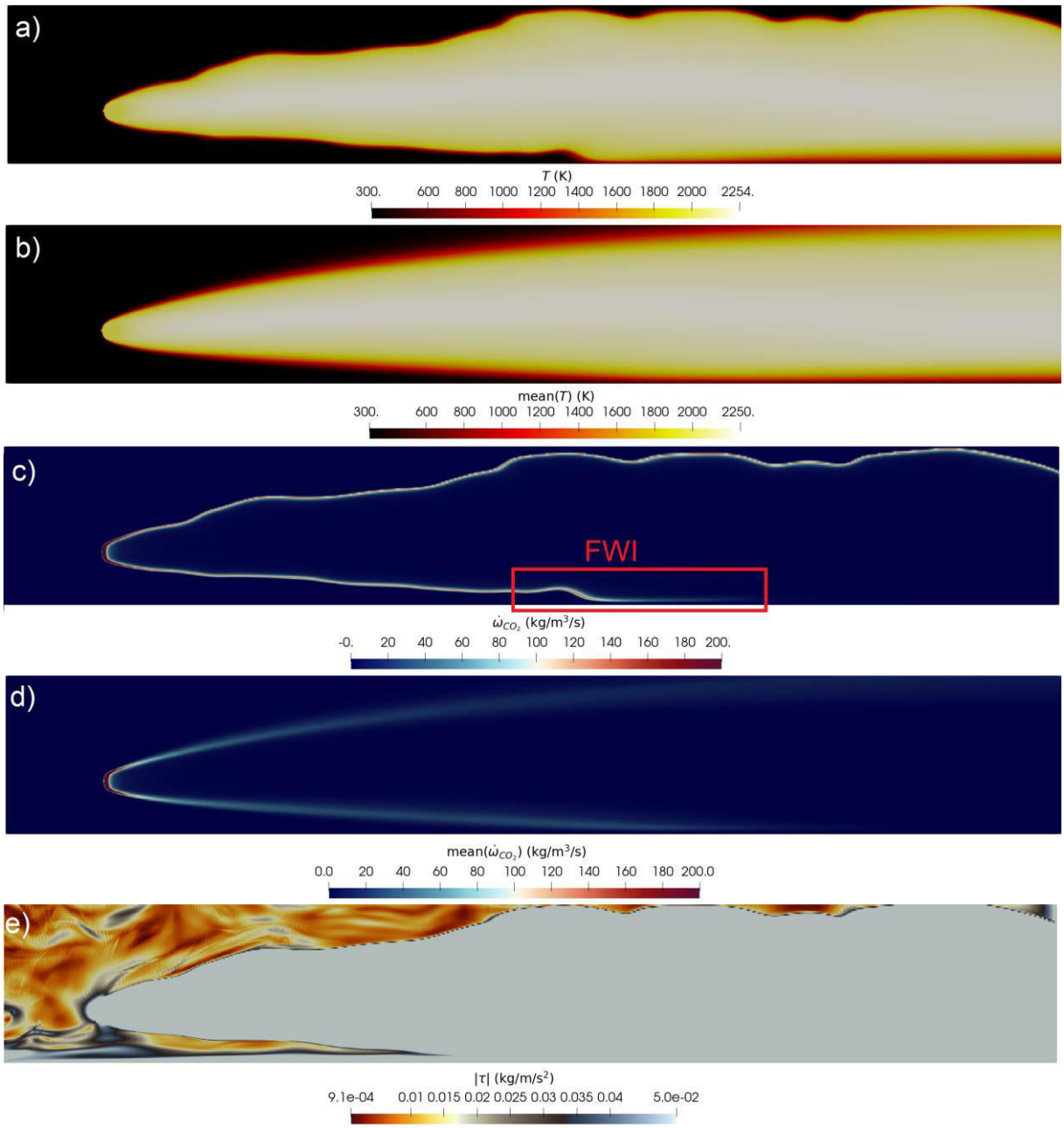

Figure 5. Different quantities on a two-dimensional cutting plane near the bottom wall of the channel. a) instantaneous temperature field; b) time-averaged temperature field; c) instantaneous reaction rate of CO_2; d) time-averaged reaction rate of CO_2; e) instantaneous magnitude of the stress tensor $\boldsymbol{\tau}$ from Eq. (3).

Figure 6 shows a close up of the mass fraction field of CO_2 (top), reaction rate of CO_2 (center) and heat release rate (bottom) in the flame-wall interaction (FWI) zone highlighted in Figure 5c. The quenching process can be clearly seen by the CO_2 reaction rate and heat release rate only being able to approach the cold wall within the quenching distance and full extinction further downstream.

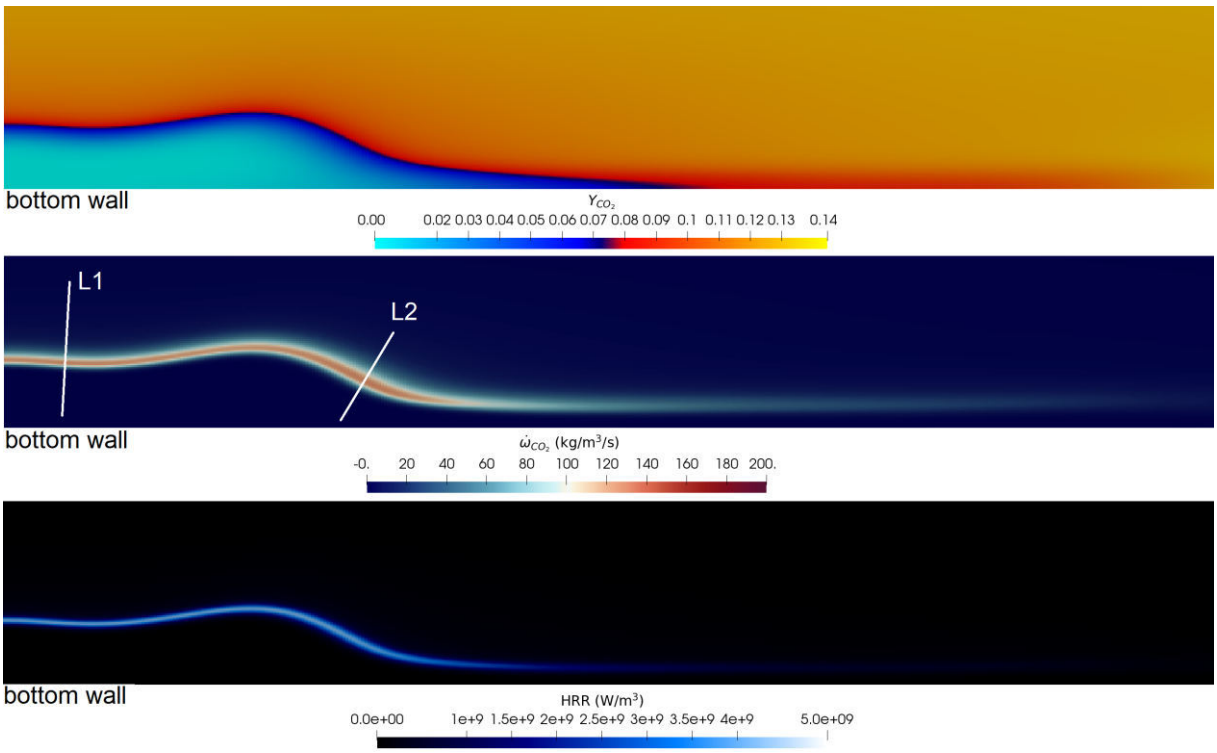

Figure 6. Zoom to different instantaneous quantities within the flame-wall interaction zone (FWI) from Figure 5. Top: mass fraction of CO_2; center: reaction rate of CO_2; bottom: heat release rate (HRR).

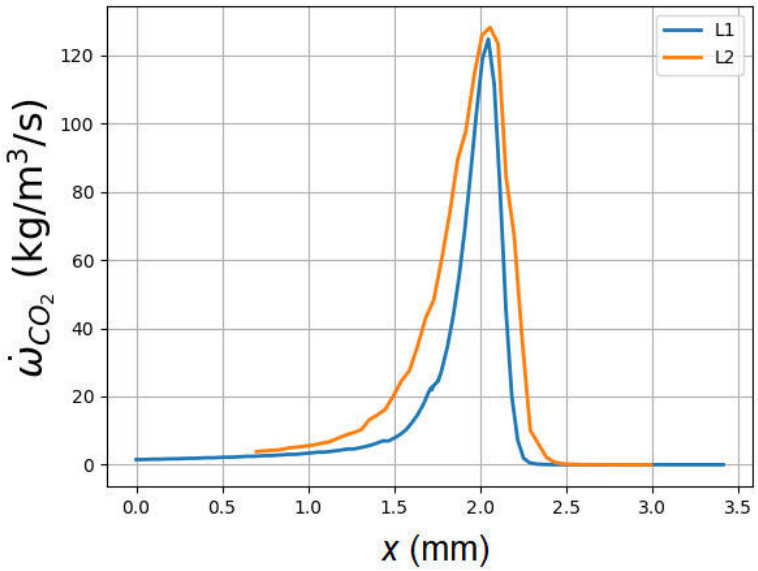

Figure 7. Profiles of the reaction rate of CO_2 along lines L1 and L2 from Figure 6 showing local broadening of the flame reaction zone.

Due to the flame's reaction zone being fully resolved, other effects can be observed as well. The CO_2 reaction rate field in Figure 6 shows that the reaction zones becomes locally broadened before the quenching point due to the unsteady interaction with the turbulent flow. Two lines are marked in Figure 6 in the center plot: Line 1 (L1) is taken perpendicular to the flame about 9 mm away from the quenching point, while line 2 (L2) is taken perpendicular to the flame front directly before the quenching point. The profile of the instantaneous reaction rate of CO_2 is plotted in Figure 7, where the local broadening can be clearly seen. These types of phenomena that require a full spatial and temporal resolution of the flame-wall interaction can be investigated with the generated data from the DNS.

Summary and Outlook

A DNS of a turbulent channel flow has been conducted, where a premixed V-shaped methane-air flame interacts with a cold wall. The flame-wall interaction in the turbulent flow is resolved with a smallest wall-normal grid resolution of 12 µm and the flame quenching process is considered with finite rate chemistry. The simulation results have been compiled into a database, that can be used for model validation and development targeting flame-wall interaction. For example, the joint PDF between reaction rates and chemical scalars or the local burning speed can be derived from the database in dependence of the flame-to-wall distance.
Currently, the database is used to test the performance of Quadrature-based Moment Methods regarding flame-wall interactions [34].

Acknowledgments

The authors gratefully acknowledge the financial support by the Helmholtz Association of German Research Centers (HGF), within the research field MTET (Materials and Technologies for the Energy Transition), subtopic "Anthropogenic Carbon Cycle" (38.05.01). The simulations have been performed on the national supercomputer HPE Apollo Hawk at the High Performance Computing Center Stuttgart (HLRS) and ForHLR II as well as HoreKa, funded by the Ministry of Science, Research and the Arts Baden-Württemberg and DFG ("Deutsche Forschungsgemeinschaft"). M. Steinhausen and C. Hasse gratefully acknowledge the support from the Deutsche Forschungsgemeinschaft (DFG, German Research Foundation)—Projektnummer 237267381—TRR 150.

References

[1] Poinsot T., Veynante D.: *Theoretical and numerical combustion*, RT Edwards, Inc., 2005.

[2] Jainski C., Rißmann M., Böhm B., Janicka J., Dreizler A.: *Sidewall quenching of atmospheric laminar premixed flames studied by laser-based diagnostics*, Combustion and Flame, 183, 271–282, 2017.

[3] Jainski C., Rißmann M., Böhm B., Dreizler A.: *Experimental investigation of flame surface density and mean reaction rate during flame–wall interaction*, Proceedings of the Combustion Institute, 36, No. 2, 1827–1834, 2017.

[4] Kosaka H., Zentgraf F., Scholtissek A., Bischoff L., Häber T., Suntz R., Albert B., Hasse C., Dreizler A.: *Wall heat fluxes and co formation/oxidation during laminar and turbulent side-wall quenching of methane and DME flames*, International Journal of Heat and Fluid Flow, 70, 181–192, 2018.

[5] Kosaka H., Zentgraf F., Scholtissek A., Hasse C., Dreizler A.: *Effect of flame-wall interaction on local heat release of methane and dme combustion in a side-wall quenching geometry*, Flow, Turbulence and Combustion, 1–18, 2019.

[6] Gruber A., Sankaran R., Hawkes E., Chen J.: *Turbulent flame-wall interaction: a direct numerical simulation study*, Journal of Fluid Mechanics, 658, 5–32, 2010.

[7] Ahmed U., Chakraborty N., Klein M.: *Scalar gradient and strain rate statistics in oblique premixed flame–wall interaction within turbulent channel flows*, Flow, Turbulence and Combustion, 106, No. 2, 701–732, 2021.

[8] Heinrich A., Ries F., Kuenne G., Ganter S., Hasse C., Sadiki A., Janicka J.: *Large eddy simulation with tabulated chemistry of an experimental sidewall quenching burner*, International Journal of Heat and Fluid Flow, 71, 95–110, 2018.

[9] Keskinen K., Giannakopoulos G., Bolla M., Koch J., Wright Y.M., Frouzakis C., Boulouchos K., Schmidt M., Böhm B., Dreizler A.: *Novel insight into engine near-wall flows and wall heat transfer using direct numerical simulations and high-fidelity experiments*, 21. Internationales Stuttgarter Symposium, Bargende M., Reuss H.C., Wagner A. (Eds.), Springer Fachmedien Wiesbaden, Wiesbaden, 377–394.

[10] OpenCFD, OpenFOAM: The Open Source CFD Toolbox. User Guide Version 1.4, OpenCFD Limited, Reading UK, Apr. 2007.

[11] Zhang F., Bonart H., Zirwes T., Habisreuther P., Bockhorn H., Zarzalis N.: *Direct numerical simulation of chemically reacting flows with the public domain code OpenFOAM*, High Performance Computing in Science and Engineering '14, Nagel W., Kröner D., Resch M. (Eds.), Springer Berlin Heidelberg, 221–236, 2015.

[12] Goodwin D., Moffat H., Speth R., *Cantera: An object-oriented software toolkit for chemical kinetics, thermodynamics, and transport processes*, 2017, http://www.cantera.org.

[13] Hindmarsh A.C., Brown P.N., Grant K.E., Lee S.L., Serban R., Shumaker D.E., Woodward C.S.: *Sundials: Suite of nonlinear and differential/algebraic equation solvers*, ACM Transactions on Mathematical Software (TOMS), 31, No. 3, 363–396, 2005.

[14] Zhang F., Zirwes T., Habisreuther P., Bockhorn H.: *A DNS Analysis of the Evaluation of Heat Release Rates from Chemiluminescence Measurements in Turbulent Combustion*, High Performance Computing in Science and Engineering '16, Nagel W., Kröner D., Resch M. (Eds.), Springer, 229–243, 2016.

[15] Zhang F., Zirwes T., Habisreuther P., Bockhorn H.: *Effect of unsteady stretching on the flame local dynamics*, Combust. Flame, 175, 170–179, 2017.

[16] Zirwes T., *Effect of stretch on the burning velocity of laminar and turbulent premixed flames*, Master's thesis, Karlsruhe Institute of Technology, 2016

[17] Zirwes T., Zhang F., Habisreuther P., Bockhorn H., Trimis D*.: Large-Scale Quasi-DNS of Mixed-Mode Turbulent Combustion*, PAMM, 19, No. 1, 2019.

[18] Zhang F., Zirwes T., Habisreuther P., Bockhorn H., Trimis D., Nawroth H., Paschereit C.O.: *Impact of combustion modeling on the spectral response of heat release in LES,* Combustion Science and Technology, 191, No. 9, 1520–1540, 2019.

[19] Zirwes T., Zhang F., Häber T., Bockhorn H.: *Ignition of combustible mixtures by hot particles at varying relative speeds*, Combust. Sci. Tech., 191, 178–195, 2019.

[20] Zirwes T., Zhang F., Habisreuther P., Hansinger M., Bockhorn H., Pfitzner M., Trimis D.: *Quasi-DNS dataset of a piloted flame with inhomogeneous inlet conditions*, Flow, Turb. and Combust., 104, 997–1027, 2019.

[21] Zirwes T., Zhang F., Habisreuther P., Hansinger M., Bockhorn H., Pfitzner M., Trimis D.: *Identification of Flame Regimes in Partially Premixed Combustion from a Quasi-DNS Dataset,* Flow, Turbulence and Combustion, 2020.

[22] Zirwes T., Häber T., Zhang F., Kosaka H., Dreizler A., Steinhausen M., Hasse C., Stagni A., Trimis D., Suntz R., Bockhorn H.: *Numerical Study of Quenching Distances for Side-wall Quenching Using Detailed Diffusion and Chemistry*, Flow, Turbulence and Combustion, 2020.

[23] Steinhausen M., Luo Y., Popp S., Strassacker C., Zirwes T., Kosaka H., Zentgraf F., Maas U., Sadiki A., Dreizler A., Hasse C.: *Numerical investigation of local heat release rates and thermo-chemical states in sidewall quenching of laminar methane and dimethyl ether flames*, Flow, Turbulence and Combustion, 2020.

[24] Hansinger M., Zirwes T., Zips J., Pfitzner M., Zhang F., Habisreuther P., Bockhorn H.: *The Eulerian stochastic fields method applied to large eddy simulations of a piloted flame with inhomogeneous inlet*, Flow, Turbulence and Combustion, 105, 837–867, 2020.

[25] Zhang F., Zirwes T., Häber T., Bockhorn H., Trimis D., Suntz R.: *Near Wall Dynamics of Premixed Flames*, Proceedings of the Combustion Institute, Vol. 38, 2020.

[26] Wang Y., Zhang H., Zirwes T., Zhang F., Bockhorn H., Chen Z.: *Ignition of dimethyl ether/air mixtures by hot particles: Impact of low temperature chemical reactions*, Proceedings of the Combustion Institute, Vol. 38, 2020.

[27] Zirwes T., Zhang F., Jordan A., Habisreuther P., Bockhorn H., Trimis D.*: Lagrangian tracking of material surfaces in reacting flows, OpenFOAM Workshop*, Vol. 15, 2020.

[28] Zirwes T., Zhang F., Denev J.A., Habisreuther P., Bockhorn H.: *Automated code generation for maximizing performance of detailed chemistry calculations in OpenFOAM*, High Performance Computing in Science and Engineering'17, Springer, 189–204, 2018.

[29] Zirwes T., Zhang F., Denev J., Habisreuther P., Bockhorn H.: *Improved vectorization for efficient chemistry computations in OpenFOAM for large scale combustion simulations*, High Performance Computing in Science and Engineering '18, Nagel W., Kröner D., Resch M. (Eds.), Springer Berlin Heidelberg, 209–224, 2018.

[30] Zirwes T., Zhang F., Denev J., Habisreuther P., Bockhorn H., Trimis D.: *Enhancing OpenFOAM's performance on HPC systems*, High Performance Computing in Science and Engineering '19, Nagel W., Kröner D., Resch M. (Eds.), Springer Berlin Heidelberg, 2019.

[31] Zirwes T., Zhang F., Habisreuther P., Denev J., Bockhorn H., Trimis D.: *Optimizing load balancing of reacting flow solvers in OpenFOAM for high performance computing*, Proc. of 6th ESI OpenFOAM User Conference, Vol. 6, 2018.

[32] Soysal M., Berghoff M., Zirwes T., Vef M., Oeste S., Brinkman A., Nagel W., Streit A.: *Using On-demand File Systems in HPC Environments*, International Conference on High Performance Computing & Simulation, 6th Special Session on High Performance Computing Benchmarking and Optimization, 2019.

[33] Ranzi E., Frassoldati A., Grana R., Cuoci A., Faravelli T., Kelley A., Law C.K.: *Hierarchical and comparative kinetic modeling of laminar flame speeds of hydrocarbon and oxygenated fuels*, Progress Energy and Combustion Science, 38, No. 4, 468–501, 2012.

[34] Steinhausen M., Zirwes T., Ferraro F., Popp S., Zhang F., Bockhorn H., Hasse C.: *Turbulent flame wall interaction of premixed flames using Quadrature-based Moment Methods (QbMM) and tabulated chemistry: an a priori analysis*, International Journal of Heat and Fluid Flow, 2021 (submitted).